Pramāṇa – J. Phys., Vol. 26, No. 4, April 1986, pp. 317–326. © Printed in India.

# Zeros of the helicity amplitudes of $\Sigma^+$–$p$ elastic scattering

S MOHANTY and J K MOHAPATRA*

Department of Physics, Utkal University, Bhubaneswar 751 004, India
* Department of Physics, Regional College of Education, Bhubaneswar 751 007, India

MS received 6 May 1985; revised 22 October 1985

**Abstract.** Optimally exploiting the analytic structure of the helicity amplitudes of $\Sigma^+$–$p$ scattering we locate their zeros by making a fit to the differential cross-section curves at 40, 100 and 150 MeV energies. Minute changes in the positions of the zeros produced detectable noises in the fit. It was observed that quite reliable predictions for the phase shifts can also be obtained from this analysis.

**Keywords.** $\Sigma^+$–$p$ elastic scattering; optimized polynomial expansion technique; helicity amplitudes; phase shifts; coupling parameters.

**PACS No.** 13·75

## 1. Introduction

In the absence of nearby poles in the helicity amplitudes of YN scattering, zeros, other than the kinematical zeros, are considered to be interesting features of the helicity amplitudes. In a recent paper (Mohanty and Mohapatra 1984), hereafter referred to as paper I, we located these zeros for $\Sigma^-$–$p$ and $\Lambda$–$p$ elastic scattering. We also observed from this analysis that one can reliably compute the phase shifts and coupling parameters between channels of fixed $J$ values.

For a long time phase shift analysis of YN scattering has remained an ill-posed practical problem because of the facts that (i) only scanty error affected data are available and (ii) one has to handle a large number of parameters in such an analysis. In fact, even at low energies around 100 MeV one has as high as 36 parameters. This leads to sets of tautological solutions. It is felt that a reduction in the number of free parameters may act as a stabilizing lever for such an analysis. In paper I, we have indicated that the phase shifts and coupling parameters can be possibly computed as a byproduct by using the zeros of the helicity amplitudes as free parameters. This was found to be an economic method in the sense that with only 18 zeros as free parameters in $\Lambda$–$p$ scattering we were able to obtain the values of 26 phase shifts and coupling parameters. In this paper we test the utility of the method for $\Sigma^+$–$p$ scattering at three fixed energies and complete this analysis for elastic YN scattering.

We map the cut $\cos\theta$ plane of analyticity of the helicity amplitudes into the interior of an ellipse. Then by using a parametrization which can see the zeros better, the zeros are located by making a least $\chi^2$ fit to the differential cross-section curve. Using changes in $\chi^2$ as indicators of the sensitiveness of the zeros towards minute changes in their positions we observed that it is difficult to obtain equally reliable different sets of zeros. We then computed the phase shifts and coupling parameters which match well with the

results of earlier workers (de Swart and Dullemond 1961; Nagels *et al* 1977, 1979).

In §2 we give our scheme of parametrization. Section 3 contains our results and concluding remarks.

## 2. Scheme of parametrization

For the scattering

$$\Sigma^+ p \to \Sigma^+ p, \tag{1}$$

the scattering amplitude has six independent helicity amplitudes, $\Phi_i$ (Jacob and Wick 1959; Lettessier and Tounsi 1971). In terms of the partial helicity amplitudes, $\phi_i^J$, the differential scattering cross-section is given by (Lettessier and Tounsi 1971)

$$\frac{d\sigma}{d\Omega} = \frac{\alpha}{2k^2} \sum_{i=1}^{6} \sum_{J=0}^{\infty} \sum_{J'=0}^{\infty} (2J+1)\,(2J'+1)\,(-1)^{\lambda-\lambda'}\,(\delta_{i5}+\delta_{i6}+1)$$

$$\phi_i^J \phi_i^{J'*} \sum_l \langle JJ', \lambda'-\lambda | 10 \rangle \langle JJ', \lambda'-\lambda | 10 \rangle P_l(\cos\theta), \tag{2}$$

where
$$\alpha = \frac{1}{(2S_{\Sigma^+}+1)(2S_p+1)} = \text{the statistical weight}, \tag{3}$$

$S_{\Sigma^+}$ is the spin of the $\Sigma^+$ hyperon, $S_p$, the spin of the proton, $k$, the length of the three-vector corresponding to the four momentum, and $l$ takes values from $|J-J'|$ to $J+J'$ (Rose 1959).

The helicity amplitudes, $\Phi_i$ have (Cohen-Tannoudji *et al* 1968) kinematical singularities in the form of zero at $\cos\theta = \pm 1$, because they can be written as

$$\Phi_i = f_{\lambda\lambda'} \Phi_i', \tag{4}$$

where

$$f_{\lambda\lambda'} = (1+\cos\theta)^{|\lambda+\lambda'|/2} (1-\cos\theta)^{|\lambda-\lambda'|/2}. \tag{5}$$

However these singularities do not affect (Cohen-Tannoudji *et al* 1968; Szego 1959) the domain of convergence of the helicity amplitudes which are completely characterized by the dynamical singularities. We call the $\Phi_i'$ as the reduced helicity amplitudes.

The $\Phi_i'$s for $\Sigma^+$–$p$ scattering are analytical in the $\cos\theta$ plane except for the cuts $x_{+\Sigma^+}$ to $\infty$ and $-x_{-\Sigma^+}$ to $-\infty$ (figure 1a) where

$$x_{+\Sigma^+} = 1 + M_p^2/k^2, \tag{6}$$

$$-x_{-\Sigma^+} = 1 - (M_\Lambda + M_p)^2/2k^2. \tag{7}$$

We symmetrize the cuts by mapping the $\underline{|}x$ plane onto the $\underline{|}w$ plane (figure 1b) where

$$W = (x_+ X_- + x_- X_+)/(X_+ + X_-), \tag{8}$$

and
$$X_\pm = (x_\pm^2 - 1)^{1/2}. \tag{9}$$

The mapped $\underline{|}w$ plane is defined by

$$w = (x - x_0)/(1 - x x_0), \tag{10}$$

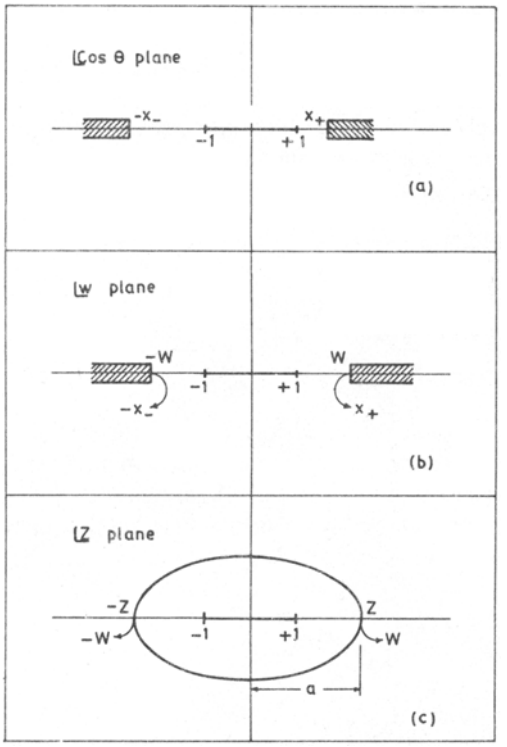


**Figure 1.** (a) Analytic structure of the scattering amplitude in $\underline{x}$ plane, $x_+$, $x_-$ are the position of the right hand and left hand cuts respectively. (b) $W$, $-W$ are the position of the cuts in the symmetrized $\underline{w}$ plane. (c) Ellipse of convergence in the mapped $\underline{z}$ plane with semi-major axis = $a$.

where $$x_0 = (x_- - x_+)/(x_+x_- + X_+X_- - 1). \tag{11}$$

The physical region $(-1, 1)$ in the $\underline{x}$ plane is then mapped onto the region $(-1, 1)$ of the $\underline{w}$ plane. The $\underline{w}$ plane is next mapped into an unifocal ellipse (figure 1c) in the $\underline{z}$ plane such that $x = \pm 1$ maps onto $z = \pm 1$, and the cuts are mapped to form the boundary of the ellipse. $z$ is given by

$$z = \sin\psi(w, \beta_0), \tag{12}$$

$$\psi(w,\beta) = \pi F(\sin^{-1} w, K)/2K(\beta), \tag{13}$$

where $F(\gamma, \beta)$ and $K(\beta) = F(\pi/2, K)$ are respectively the incomplete and complete elliptic integrals of the first kind and $\beta_0 = 1/W$. The mapping from the symmetrized $\underline{w}$ plane to an unifocal ellipse is chosen because at low energies, this mapping tends to maximize the rate of convergence, given by

$$R = a + (a^2 - 1)^{1/2}, \tag{14}$$

$a$ being the semi-major axis of the ellipse (figure 1c). This mapping has been successfully used by many workers (Cutkosky and Deo 1968b; Shih 1971; Deo and Mohapatra 1982) for low energy data analysis of various scattering processes.

We now represent the six reduced helicity amplitudes, $\Phi'_i$s as

$$\Phi'_i = \Phi'_{iR} + i\Phi'_{iI}, \tag{15}$$

where $\Phi'_{iR}$ and $\Phi'_{iI}$ are respectively the real and imaginary parts of the reduced helicity amplitudes. Assuming that there is at least one dynamical zero in each of these $\Phi'_{iR}$ and $\Phi'_{iI}$, we write them in the following polynomial form

$$\Phi'_{iR} = (z - Z^i_{0R}) \sum_{n=0}^{\infty} a_{in} T_n(z), \tag{16}$$

$$\Phi'_{iI} = (z - Z^i_{0I}) \sum_{n=0}^{\infty} b_{in} T_n(z), \tag{17}$$

where $T_n(z)$ is the Chebyseff polynomial of order $n$, $Z_{0R}$ and $Z_{0I}$ are the positions of the zeros of the corresponding amplitudes. $T_n(z)$ has been used in this expansion as its figure of convergence is an ellipse and coincides with the domain of analyticity of the amplitudes in the $\underline{z}$ plane, and so a suitably truncated series will still be a faithful representation of the actual amplitudes in so far as the fit to the data is concerned.

## 3. Results and conclusion

After constructing the helicity amplitudes, (16) and (17) as polynomials in the mapped $z$ variable the differential cross-sections were calculated by using (2) and were fitted to the curves (de Swart and Dullemond 1961) for $\Sigma^+$–$p$ scattering at 40 MeV, 100 MeV and 150 MeV. We note here that due to the very low probability of the production of $\Sigma^+$ hyperon $\Sigma^+$–$p$ scattering has not attracted much attention of even the experimenters. So in the absence of any recently published number for experimental differential cross-section we took the old curves of de Swart and Dullemond (1961) as our data with an average error of 10% at every data point. And as our aim is to check the correctness of our conjecture that an analysis of the dynamical zeros can lead to reliable values for the phase shifts, even this old data will serve our purpose. Further since the data are scanty this analysis will also have the scope to exhibit its degree of utility. We have not considered the effect of Coulomb interaction as it is negligible (Helder 1967) for this range of energies.

By the $\chi^2$ minimization technique we tried to search for the parameters in (16) and (17) to obtain a reliable fit to the $\Sigma^+$–$p$ scattering cross-section data at 40 MeV, 100 MeV and 150 MeV. It was heartening to note that only one zero (table 1a) in each of the $\Phi'_{iR}$ and $\Phi'_{iI}$ and just the constant terms (table 1b) in the polynomial expansion were enough to obtain a good fit to the data. Our best fit curves are given in figure 2. The corresponding $\chi^2$/NDF values for 40, 100 and 150 MeV are 0·3, 0·2 and 0·2 respectively. Because of these low values for $\chi^2$/NDF our fits are expected to be reliable. These zeros lie on the semi-major axes of the ellipses because at 40, 100 and 150 MeV the energy-dependent semi-major axis has values 210·04, 85·10 and 57·46. It is clear from table 1a that the zeros are moving with energy. In particular the zeros of $\Phi'_{1R}$, $\Phi'_{2R}$, $\Phi'_{3R}$ and $\Phi'_{6I}$ move from left to right in the $\underline{z}$ plane whereas the zeros of all the rest of the partial helicity amplitudes move from right to left. As a result of this energy-dependent motion of the zeros $\Phi'_{5R}$, $\Phi'_{6R}$ are in the physical region at 150 MeV, although they were in the

**Table 1a.** Position of the zeros of the helicity amplitudes for 40 MeV, 100 MeV and 150 MeV.

| Helicity amplitude zeros | Scattering energies | | |
|---|---|---|---|
| | 40 MeV | 100 MeV | 150 MeV |
| $Z^1_{0R}$ | $-3{\cdot}8 \pm 0{\cdot}01$ | $-1{\cdot}65 \pm 0{\cdot}02$ | $-1{\cdot}41 \pm 0{\cdot}18$ |
| $Z^2_{0R}$ | $-0{\cdot}01 \pm 0{\cdot}01$ | $0{\cdot}39 \pm 0{\cdot}07$ | $0{\cdot}43 \pm 0{\cdot}05$ |
| $Z^3_{0R}$ | $-1{\cdot}41 \pm 0{\cdot}03$ | $-1{\cdot}49 \pm 0{\cdot}01$ | $-1{\cdot}53 \pm 0{\cdot}04$ |
| $Z^4_{0R}$ | $-6{\cdot}77 \pm 1{\cdot}5$ | $-1{\cdot}38 \pm 0{\cdot}25$ | $-1{\cdot}33 \pm 0{\cdot}33$ |
| $Z^5_{0R}$ | $1{\cdot}18 \pm 0{\cdot}25$ | $0{\cdot}69 \pm 0{\cdot}6$ | $0{\cdot}59 \pm 0{\cdot}5$ |
| $Z^6_{0R}$ | $1{\cdot}17 \pm 0{\cdot}2$ | $0{\cdot}57 \pm 0{\cdot}5$ | $0{\cdot}54 \pm 0{\cdot}5$ |
| $Z^1_{0I}$ | $1{\cdot}69 \pm 0{\cdot}13$ | $1{\cdot}44 \pm 0{\cdot}12$ | $1{\cdot}36 \pm 0{\cdot}12$ |
| $Z^2_{0I}$ | $1{\cdot}71 \pm 0{\cdot}6$ | $1{\cdot}44 \pm 0{\cdot}13$ | $1{\cdot}37 \pm 0{\cdot}12$ |
| $Z^3_{0I}$ | $-1{\cdot}32 \pm 0{\cdot}6$ | $-1{\cdot}47 \pm 0{\cdot}25$ | $-1{\cdot}50 \pm 0{\cdot}13$ |
| $Z^4_{0I}$ | $-1{\cdot}73 \pm 0{\cdot}05$ | $-1{\cdot}87 \pm 0{\cdot}33$ | $-1{\cdot}94 \pm 0{\cdot}2$ |
| $Z^5_{0I}$ | $21{\cdot}15 \pm 21$ | $-3{\cdot}31 \pm 2{\cdot}9$ | $-3{\cdot}43 \pm 3$ |
| $Z^6_{0I}$ | $-25{\cdot}41 \pm 25$ | $-6{\cdot}22 \pm 6$ | $-4{\cdot}8 \pm 4$ |

**Table 1b.** Values of $a_{in}$ and $b_{in}$ of the helicity amplitudes.

| Constant terms | Scattering energies | | |
|---|---|---|---|
| | 40 MeV | 100 MeV | 150 MeV |
| $a_{10}$ | 0·52931 | 0·95274 | 0·92101 |
| $a_{20}$ | −1·1397 | −0·99822 | −0·98328 |
| $a_{30}$ | −0·57637 | −0·47836 | −0·49118 |
| $a_{40}$ | −0.04513 | 0·32326 | 0·32035 |
| $a_{50}$ | −0·39025 | −0·2702 | −0·25081 |
| $a_{60}$ | −0·39756 | −0·27173 | −0·25366 |
| $b_{10}$ | 0·42528 | 0·41528 | 0·4026 |
| $b_{20}$ | 0·41899 | 0·40658 | 0·39411 |
| $b_{30}$ | 0·16215 | 0·33419 | 0·3428 |
| $b_{40}$ | 0·14109 | 0·20787 | 0·19861 |
| $b_{50}$ | 0·00453 | −0·04036 | −0·04968 |
| $b_{60}$ | −0·00353 | −0·02131 | −0·02967 |

unphysical region at 40 MeV. It is conjectured that at higher energies the zeros of $\Phi'_{1R}$, $\Phi'_{4R}$, $\Phi'_{1I}$, $\Phi'_{2I}$ and $\Phi'_{6I}$ may also enter into the physical region.

We then tried to change the positions of the zeros and examine the corresponding changes in $\chi^2$. Our results for the zeros of $\Phi'_{1R}$, $\Phi'_{2R}$, $\Phi'_{1I}$ and $\Phi'_{2I}$ for 40 MeV, 100 MeV and 150 MeV are shown in figure 3.

Similar effects were observed when the positions of the other zeros were varied. Although we are unable to prove the uniqueness of the positions of the zeros arrived at by us, figure 3 demonstrates that it will be difficult to obtain tautological sets of zeros by this procedure.

After obtaining the best values for the position of zeros, we tried to test our conjecture that the phase shifts and coupling parameters can possibly be predicted

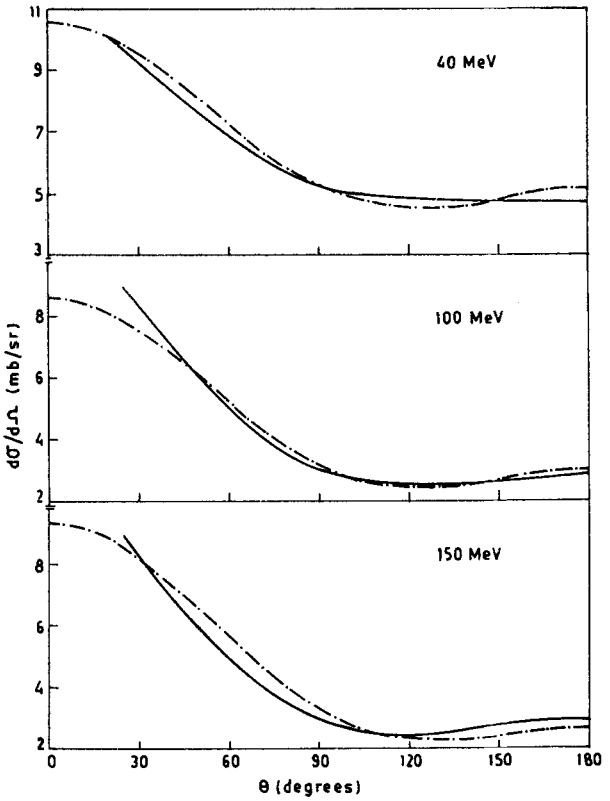


**Figure 2.** Differential cross-section curves at $E_{lab}$ = 40 MeV, 100 MeV and 150 MeV $\Sigma^+$–$p$ scattering. (—. —. —) Present analysis and (——) analysis of de Swart and Dullemond (1971).

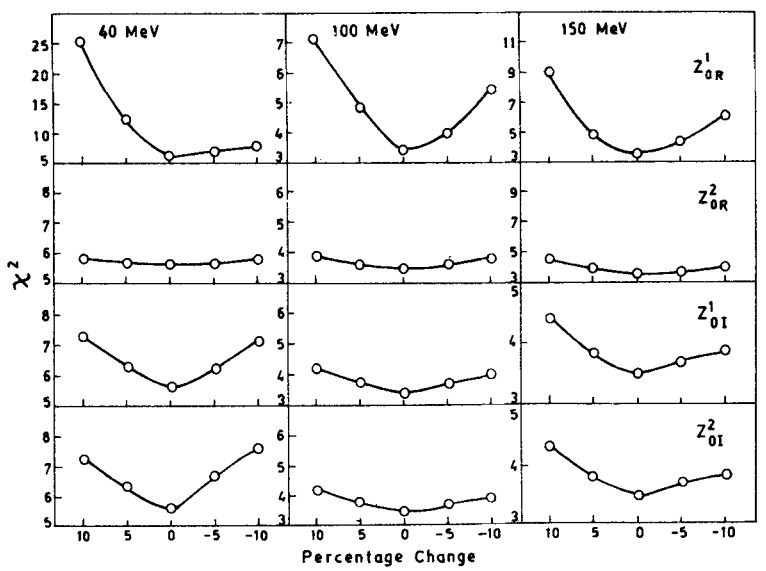


**Figure 3.** Effect of changes in $Z^1_{0R}$, $Z^2_{0R}$, $Z^1_{0I}$ and $Z^2_{0I}$ on $\chi^2$ for 40 MeV, 100 MeV and 150 MeV.

accurately. Once the helicity amplitudes are constructed, partial helicity amplitudes $\phi^J_{iR}$ and $\phi^J_{il}$ can be projected out by exploiting the orthogonality property of the reduced rotation matrix (Jacob and Wick 1959). Using the $\phi^J_i$'s we calculated the elements of the reaction matrix $R$ (Lettessier and Tounsi 1971). The $S$ matrix can be diagonalized by a real and unitary matrix $U$ and

$$S^J = U^{-1}\Delta U \tag{18}$$

where $\Delta$ is also unitary and depends on $n$ real phase shifts $\delta_j$, ($j = 1, 2, \ldots n$) defined by

$$\Delta_{jj} = \exp[2i\delta_j], \tag{19}$$

and

$$U = \begin{vmatrix} \cos\varepsilon & \sin\varepsilon \\ -\sin\varepsilon & \cos\varepsilon \end{vmatrix}, \tag{20}$$

$\varepsilon$ being the coupling parameter. The phase shifts and coupling parameters as obtained from this analysis are given in tables 2–4. The eigen phase shifts and coupling parameters are labelled by well-defined values of $J$, $l$ and $2S + 1$. For example the phase shift corresponding to $S = 0$, $l = 1$, $J = 1$ is designated by $^1P_1$, and $S = 1$, $l = 0$ and $J = 1$ by $^3S_1$. Similarly the coupling parameter is labelled by definite $S$ and $J$ values. For example the coupling between the singlet and triplet states for $J = 1$ is denoted by $^1\varepsilon_1$ and that between the triplet and triplet states for $J = 1$ is by $^3\varepsilon_1$. These phase shifts and

**Table 2.** Eigen phase shifts and coupling parameters in degrees for 40 MeV.

| Phase shifts and coupling parameters | Present value 40 MeV | de Swart and Dullemond (1971) 40 MeV | Nagels (1977) 37·2 MeV |
|---|---|---|---|
| $^1S_0$ | 33·8 | 55·5 | 31·58 |
| $^3P_0$ | 34·4 | 10·7 | 8·8 |
| $^1P_1$ | 8·5 | 11·0 | 26·18 |
| $^1\varepsilon_1$ | 0·08 | 0·0 | −0·15 |
| $^3P_1$ | −9·8 | −7·0 | −5·09 |
| $^1D_2$ | 0·003 | 0·8 | 0·96 |
| $^1\varepsilon_2$ | −0·32 | 0·0 | 0·0 |
| $^3D_2$ | −3·2 | −1·1 | −1·2 |
| $^1F_3$ | 0·00009 | 0·1 | 0·22 |
| $^1\varepsilon_3$ | 0·001 | 0·0 | 0·0 |
| $^3F_3$ | 0·65 | −0·1 | −0·34 |
| $^3S_1$ | −17·1 | −17·3 | −12·43 |
| $^3\varepsilon_1$ | 8·2 | 14·3 | 14·53 |
| $^3D_1$ | 0·3 | 1·9 | 1·75 |
| $^3P_2$ | 1·8 | 4·6 | −3·21 |
| $^3\varepsilon_2$ | −7·9 | −13·7 | 1·35 |
| $^3F_2$ | −2·1 | −0·2 | 0·16 |
| $^3D_3$ | −0·66 | 0·4 | 0·33 |
| $^3\varepsilon_3$ | 41·0 | −17·7 | – |
| $^3G_3$ | −0·00003 | – | – |

**Table 3.** Eigen phase shifts and coupling parameters in degrees for 100 MeV.

| Phase shifts and coupling parameters | Present values 100 MeV | de Swart and Dullemond (1971) 100 MeV | Nagels (1977) 100·8 MeV |
|---|---|---|---|
| $^1S_0$ | 31·2 | 36·4 | 14·60 |
| $^3P_0$ | 27·0 | 10·5 | 8·14 |
| $^1P_1$ | 16·6 | 25·5 | 21·25 |
| $^1\varepsilon_1$ | −0·31 | 0·0 | −0·20 |
| $^3P_1$ | −20·4 | −13·7 | −9·92 |
| $^1D_2$ | 0·013 | 3·5 | 3·68 |
| $^1\varepsilon_2$ | −0·77 | 0·0 | −0·17 |
| $^3D_2$ | −0·58 | −1·0 | −2·95 |
| $^1F_3$ | 0·0004 | 0·8 | 0·88 |
| $^1\varepsilon_3$ | −0·008 | 0·0 | 0·00 |
| $^3F_3$ | −1·11 | −1·2 | −1·20 |
| $^1G_4$ | 0·00008 | 0·2 | 0·83 |
| $^1\varepsilon_4$ | −0·00002 | 0·0 | 0·0 |
| $^3G_4$ | 0·09 | 0·0 | 0·0 |
| $^3S_1$ | −14·2 | −28·3 | −24·35 |
| $^3\varepsilon_1$ | 20·6 | 13·4 | 11·38 |
| $^3D_1$ | 0·55 | 3·5 | 3·08 |
| $^3P_2$ | 0·85 | 13·4 | 8·69 |
| $^3\varepsilon_2$ | −28·4 | −13·7 | −15·97 |
| $^3F_2$ | −5·0 | −0·2 | 0·05 |
| $^3D_3$ | 0·22 | 3·3 | 2·38 |
| $^3\varepsilon_3$ | 38·9 | −20·3 | −24·99 |
| $^3G_3$ | −0·0001 | −0·3 | −0·22 |
| $^3F_4$ | −0·06 | 0·5 | 0·67 |
| $^3\varepsilon_4$ | 41·8 | −34·3 | −32·52 |

coupling parameters are compared with the values of earlier workers (de Swart and Dullemond 1961; Nagels *et al* 1977, 1979). In doing these comparisons we were careful to convert the nuclear bar phase shifts of Nagels *et al* (1977, 1979) to eigen phase shifts (Pal 1982). Our $^3P_0$ phase shift is of much high value in comparison to those workers, but Lettessier and Tounsi (1971) have also got a high value for it. We have considered the coupling between the singlet and triplet phase shifts for $J = l$ like Lettessier and Tounsi (1971) and they are given in tables 2 to 4.

In conclusion we remark that we have obtained the zeros of the helicity amplitudes of $\Sigma^+$–$p$ scattering through a bias-free method. Attempts can also be made to locate these zeros by applying such techniques as Pade approximants. However, since we have optimally used the analytic structure of the helicity amplitudes to locate the zeros, and this analytic structure reflects the forces responsible for the scattering, we hope that the location of these zeros are not dependent upon the specific parametrization chosen by us. Again the fit is very sensitive to changes in position of the zeros and so the procedure is fairly stable in the sense that it will be difficult to obtain equivalent sets of solutions for the position of zeros. Further we also conclude that an analysis of the zeros can lead to reliable prediction of the phase shifts and coupling parameters. We also note that

**Table 4.** Eigen phase shifts and coupling parameters in degrees for 150 MeV.

| Phase shifts and coupling parameters | Present values 150 MeV | de Swart and Dullemond (1977) 150 MeV | Nagels (1977) 142·8 MeV | Nagels (1979) 142·8 MeV |
|---|---|---|---|---|
| $^1S_0$ | 30·1 | 25·6 | 5·66 | 7·07 |
| $^3P_0$ | 25 | 6·6 | 4·39 | 3·9 |
| $^1P_1$ | 20·8 | 32·2 | 15·45 | 23·6 |
| $^1\varepsilon_1$ | −0·21 | 0·0 | −0·21 | 0·0 |
| $^3P_1$ | −25·6 | −17·7 | −12·54 | −18·46 |
| $^1D_2$ | 0·02 | 5·8 | 5·79 | 4·62 |
| $^1\varepsilon_2$ | −1·7 | 0·0 | −0·18 | 0·0 |
| $^3D_2$ | −0·48 | −5·5 | −3·75 | −5·47 |
| $^1F_3$ | 0·033 | 1·5 | 1·43 | 1·39 |
| $^1\varepsilon_3$ | −0·025 | 0·0 | −0·18 | 0·0 |
| $^3F_3$ | −0·25 | −2·2 | −1·62 | −2·14 |
| $^1G_4$ | 0·03 | −0·5 | 0·33 | 0·57 |
| $^1\varepsilon_4$ | −0·025 | 0·0 | 0·0 | 0·0 |
| $^3G_4$ | 0·11 | −0·8 | −0·52 | −0·98 |
| $^3S_1$ | −16·3 | −35·2 | −30·77 | −44·12 |
| $^3\varepsilon_1$ | 23·9 | 11·8 | 9·68 | 9·77 |
| $^3D_1$ | 1·0 | 3·4 | 3·05 | 2·67 |
| $^3P_2$ | 0·86 | 18·4 | 10·05 | 5·62 |
| $^3\varepsilon_2$ | −30·2 | −10·9 | −16·02 | −36·90 |
| $^3F_2$ | −6·2 | 0·4 | 0·29 | −1·46 |
| $^3D_3$ | 0·18 | 7·3 | 8·69 | 2·73 |
| $^3\varepsilon_3$ | 40·6 | −15·3 | −22·62 | −34·94 |
| $^3G_3$ | 0·0006 | −0·2 | −0·17 | −0·69 |
| $^3F_4$ | −0·18 | 1·3 | 1·11 | 1·16 |
| $^3\varepsilon_4$ | 42·5 | −32·8 | −29·03 | −33·56 |
| $^3H_4$ | 0·0009 | −0·4 | – | – |
| $^3G_5$ | 0·07 | 0·3 | – | – |

since no increase in the number of zeros (i.e. number of free parameters) was observed as the energy was increased from 40 MeV to 150 MeV, this number will possibly not increase too much as data at higher energies will be available for analysis and hence will provide an economic way for computing the phase shifts and coupling parameters of $\Sigma^+$–$p$ scattering.

## Acknowledgements

One of us (SM) thanks UGC, New Delhi, for partly financing this work. We are grateful to Prof. B B Deo for helpful suggestions, and to the Computer Centre of Utkal University for the computational facilities.

## References

Cohen-Tannoudji G, Morel A and Navelet H 1968 *Ann. Phys.* **46** 239
Cutkosky R E and Deo B B 1968a *Phys. Rev.* **174** 1859

Cutkosky R E and Deo B B 1968b *Phys. Rev. Lett.* **20** 1272
Deo B B and Mohapatra J K 1982 *Pramana (J. Phys.)* **1** 39
de Swart J J and Dullemond C 1961 *Ann. Phys.* **16** 203
Helder J C 1967 *On sigma nucleon interaction*, Thesis, University of Nigmegen, Nigmegen
Jacob M and Wick G C 1959 *Ann. Phys.* **7** 404
Lettessier J and Tounsi A 1971 *Nuovo Cimento* **A5** 56
Mohanty S and Mohapatra J K 1984 *Pramana (J. Phys.)* **23** 475
Nagels M M, Rijken T A and de Swart J J 1977 *Phys. Rev.* **D15** 2547
Nagels M M, Rijken T A and de Swart J J 1979 *Phys. Rev.* **D20** 1633
Pal M K 1982 *Theory of nuclear structure* (New Delhi: East West Press)
Rose M E 1959 *Elementary theory of angular momentum* (New York: John Wiley)
Shih C C 1971 *Phys. Rev.* **D4** 3293
Szego G 1959 *Orthogonal polynomials* (American Physical Society) Vol. 23